Bioorganic & Medicinal Chemistry Letters 21 (2011) 2898–2905

Contents lists available at ScienceDirect

Bioorganic & Medicinal Chemistry Letters

journal homepage: www.elsevier.com/locate/bmcl

Pharmacophore elucidation for a new series of 2-aryl-pyrazolo-triazolo-pyrimidines as potent human A_3 adenosine receptor antagonists

Siew Lee Cheong [a], Stephanie Federico [b], Gopalakrishnan Venkatesan [a], Priyankar Paira [a], Yi-Ming Shao [a], Giampiero Spalluto [b], Chun Wei Yap [c,*], Giorgia Pastorin [a,*]

[a] Department of Pharmacy, National University of Singapore, 3 Science Drive 2, Block S15, #05-PI-03, Singapore 117543, Singapore
[b] Dipartimento di Scienze Farmaceutiche, Università degli Studi di Trieste, Piazzale Europa 1, I-34127 Trieste, Italy
[c] Department of Pharmacy, National University of Singapore, 18 Science Drive 4, Block S7, #02-06, Singapore 117543, Singapore

ARTICLE INFO

Article history:
Received 19 February 2011
Revised 17 March 2011
Accepted 18 March 2011
Available online 26 March 2011

Keywords:
hA_3 Adenosine receptor antagonists
2-Aryl-pyrazolo-triazolo-pyrimidine
QSAR
CoMFA

ABSTRACT

A ligand-based pharmacophore was obtained for a new series of 2-unsubstituted and 2-(*para*-substituted)phenyl-pyrazolo-triazolo-pyrimidines as potent human A_3 adenosine receptor antagonists. Through comparative molecular field analysis-based quantitative structure–activity relationship studies, structural features at the N^5-, N^8- and C^2-positions of the tricyclic nucleus were deeply investigated, with emphasis given to the unprecedentedly explored C^2-position. The resulting model showed good correlation and predictability ($r^2 = 0.936$; $q^2 = 0.703$; $r^2_{pred} = 0.663$). Overall, the contribution of steric effect was found relatively more predominant for the optimal interaction of these antagonists to the human A_3 receptor.

Adenosine is an endogenous nucleoside that mediates a wide range of physiological responses through interaction with specific adenosine receptors. These receptors, which consist of 7 transmembrane domains, belong to the G protein-coupled receptor (GPCR) superfamily. There are four main types of human adenosine receptors (hARs) that have been cloned and pharmacologically characterized, namely A_1, A_{2A}, A_{2B} and A_3 ARs.[1] Each of these adenosine receptors has its own distinct biochemical pathways and pharmacological profiles. In the context of hA_3AR, the activation of such receptor subtype mediates adenylyl cyclase inhibition through the coupling with G_i protein, followed by subsequent decrease in the level of cyclic adenosine monophosphate (cAMP).[2] Besides that, other signaling pathways involving phospholipase C and D, Ca^{2+} and mitogen-activated protein kinase (MAPK) have also been associated with the activation of such receptor.[3,4] Through the above-mentioned signalling pathways, the modulation of hA_3AR receptor is thus implicated in cerebroprotective and cardioprotective functions, as well as influence on cellular growth.[5–7] On the other hand, its inhibition by selective antagonists has been reported to be potentially useful in the treatment of pathological conditions including glaucoma, inflammatory diseases and cancer.[8,9] To-date, numerous hA_3 agonists and antagonists have been proposed, and several classes of derivatives showing good hA_3 affinity and a broad range of selectivity against other receptor subtypes have been successfully synthesized and tested as hA_3AR ligands.

Among the structures that are able to inhibit the hA_3 receptor, the series of pyrazolo-triazolo-pyrimidines (PTPs), bearing different substituents at the N^5- and N^8-positions, has been identified as highly potent and moderately selective hA_3AR antagonists.[10,11] Recently, our group has designed and synthesized a new series of PTPs bearing a (*para*-(un)substituted)-phenyl ring at C^2, while maintaining either methyl or phenyl–ethyl groups at the N^8 and a phenylacetamide or benzamide at the N^5 position.[12] We have attempted to investigate the effect of a different substitution, other than the commonly adopted 2-furyl ring at the C^2-position, to increase the affinity at hA_3 receptor and the selectivity over other adenosine receptor subtypes. Based on the binding assay results, such new 2-aryl PTP derivatives demonstrated good affinity towards hA_3 receptor and significantly improved selectivity profile against the hA_1, hA_{2A} and hA_{2B} receptors as compared to the 2-furyl-PTP counterparts.[12] With the aim to clarify the structural basis

Abbreviations: CoMFA, comparative molecular field analysis; cAMP, cyclic adenosine monophosphate; ECL2, extracellular loop 2; GPCR, G protein-coupled receptor; hA_3AR, human A_3 adenosine receptor; MAPK, mitogen-activated protein kinase; MOE, molecular operating environment; PLS, partial-least-square; PQ, pyrazoloquinolines; PTP, pyrazolo-triazolo-pyrimidines; TBT, triazolobenzotriazinones; TM, transmembrane; TP, triazolopyrazinones; TQX, triazoloquinoxalinones.

* Corresponding authors. Tel.: +65 6516 5971; fax: +65 6779 1554 (C.W.Y.); tel.: +65 6516 1876; fax: +65 6779 1554 (G.P.).
E-mail addresses: phayapc@nus.edu.sg (C.W. Yap), phapg@nus.edu.sg (G. Pastorin).

0960-894X/$ - see front matter © 2011 Elsevier Ltd. All rights reserved.
doi:10.1016/j.bmcl.2011.03.073

at the N^5, N^8 and particularly at the C^2-aryl ring of the PTP tricyclic nucleus that are associated with the selective inhibition of hA_3AR, a quantitative structure–activity relationship (QSAR) study was therefore conducted. In our investigations, we employed comparative molecular field analysis (CoMFA) for such QSAR study.

A total of 83 structurally related compounds[13–20] (*training set*, **1–83** in Table 1) were selected and used to generate a CoMFA model. They consisted of six classes of polyheterocycles, namely pyrazolo-triazolo-pyrimidines (PTPs) (**1–53**); CGS15943 and its derivatives (**54–56**); triazoloquinoxalinones (TQXs) (**57–72**); pyrazoloquinolines (PQs) (**73–75**); triazolopyrazinones (TPs) (**76–79**) and triazolobenzotriazinones (TBTs) (**80–83**), all of which have been reported as potent hA_3 receptor antagonists. They were chosen in such a way that their hA_3K_i were uniformly distributed in the range of values (spanning four orders of magnitude from 10^{-2} to 10^2 nM) so that the model's predictive power could be effectively evaluated.

The rationale of adopting five additional groups of derivatives in our QSAR study, apart from the PTPs, was based on three main considerations: (1) these groups of compounds comprise similar tricyclic scaffolds (highlighted in red circles, Table 1) as that of PTPs, which are planar in shape and possess a 'pseudoaromatic' character with electrons delocalized within the three-membered-ring core; (2) these derivatives share similar substituents at the corresponding N^5/N^4-position of the tricyclic nuclei as that of 2-aryl-PTP derivatives, such as amino (NH_2), benzamidic (Ph-CONH), and phenylacetamidic (Ph-CH_2-CONH) groups; (3) most importantly, the majority of these compounds bear a similar (un)substituted-phenyl ring at the position equivalent to that of 2-aryl-PTP compounds (e.g., 2-phenyl ring found in TQX, PQ, TP, TBT derivatives). This last aspect enables the evaluation of relative importance of the aromatic ring in the 2-aryl-PTPs towards hA_3 affinity, which represents the first attempt to identify the structural requirements at the unprecedentedly explored C^2-position of PTP tricyclic nucleus. Explicitly, the inclusion of these 2-aryl group-bearing derivatives in the *training set* of our study has allowed the investigation on the significance of steric and electrostatic effects of other substituents (besides 2-furyl ring) at the C^2-position of tricyclic nuclei towards the hA_3 binding affinity; on the contrary, this is lacking in the CoMFA model previously reported by Moro et al.[21] that adopted mainly the 2-furyl PTP derivatives as hA_3AR antagonists in their study.

In CoMFA, a correct structural alignment of compounds is crucial to the success of constructing a reliable QSAR model.[22] The final alignment of all compounds (in *training* and *testing set*) was subjected to the CoMFA, and the so-obtained contour plots derived from the analysis were used to identify the relative importance of steric and electrostatic effects of substituents at the corresponding N^8, N^5/N^4 or C^2/N^2 positions (in each class of derivatives) towards the hA_3 affinity. Further interpretation of the results led to the generation of a 3-D pharmacophore map not only for the compounds in the *training set*, but most importantly, also for the new series of 2-aryl-PTPs (*testing set*, compounds **84–105** in Table 1) that presented similar tricyclic nucleus and substitutents as those in the *training set*. Furthermore, the predictive power of such CoMFA model was validated through evaluation on a number of new 2-aryl-PTPs. To further examine the predictability of the model on the *testing set*, a few rigorous criteria (including coefficient of determination and slope of regression lines when forcing the intercept through origin)[23] were also determined in this part of the study.

The final structural alignment of all compounds in *training set* and *testing set*, as shown in Figure 1, was used as input for the QSAR investigation through CoMFA. The statistical results of the generated QSAR model were reported in Table 2 and the graph showing the correlation between the experimental and predicted hA_3pK_i of compounds in the *training* set was represented in Figure 2. Cross-validated partial-least-square (PLS) analysis from CoMFA gave a correlation with cross-validated r^2 (q^2) of 0.703 and an optimum number of components set equal to 10, based on the analysis of 83 compounds in the *training set*. Subsequently, the non-cross-validated PLS analysis was repeated with the optimum number of components to give a r^2 of 0.936 (Fig. 2). The q^2 value of 0.703 indicated that the predictability of CoMFA model was considerably high. Moreover, the relatively small estimated standard error of 0.332 and a high *F*-test value of 104.782 (values obtained from non-cross-validation analysis of CoMFA) also suggested a high degree of confidence in the analysis. On top of that, the steric and electrostatic field contributions of compounds in the *training set* were shown to be 53.9% and 46.1%, respectively. Such finding indicated that the contribution of steric effect was relatively more predominant for the optimal interaction of these antagonists to the hA_3 receptor.

Although high value of q^2 (from internal validation via cross-validation) appears to be a necessary requisite, it is not sufficient to confirm that the model has high predictive power. In fact, external validation is considered fundamental to establish a reliable QSAR model.[24] Hence, in order to externally validate the predictive power of the CoMFA model constructed, 22 derivatives (compounds **84–105**) consisting of the new series of 2-(*para*-substituted)phenyl-pyrazolo-triazolo-pyrimidines were included as *testing set*, which were never used in the *training set* during the model development. The actual and predicted hA_3pK_i for this external *testing set* were shown in Table 3, and the corresponding correlation graph for predicted pK_i versus actual pK_i was illustrated in Figure 3. Consistently, the CoMFA model has shown a reasonable external predictability of $r^2_{pred} = 0.663$, which further supported the reliability of this model. In addition, predicted and actual affinities of the *testing set* were also used to calculate another set of rigorous parameters, including the coefficient of determination (R_0^2 and $R_0'^2$) and the slope of regression lines when forcing the intercept through origin (K and K') (Table 2). The obtained parameters satisfied the conditions stipulated by Tropsha et al.:[23] (a) $(r^2_{pred} - R_0^2)/(r^2_{pred}) < 0.1$ and $0.85 \leqslant K \leqslant 1.15$; (b) $|R_0^2 - R_0'^2| < 0.3$, which again substantiated the predictive power of our QSAR model. Therefore, the so-obtained QSAR model was deduced to be reliable in predicting the hA_3 affinity for the new 2-aryl PTP derivatives, and the corresponding pharmacophore map elucidated by the model was conceivably valid and applicable for such new series of PTPs.

The overall graphical representations of the analysis comprising both the electrostatic and steric contour plots were depicted in Figure 4a and b, through illustration by one of the PTP (compound **3**) and TQX (compound **71**) derivatives, respectively. Through interpretation of these contour plots, the steric and electrostatic effects at N^5-, N^8- and particularly C^2-position of the PTP tricyclic nucleus, as well as other closely related tricyclic scaffolds as mentioned earlier were elaborated in the next sections. For CoMFA steric contour, green colour indicates bulky groups are favoured for hA_3 affinity while yellow indicates bulky groups are disfavoured. In the case of electrostatic contour, red colour indicates electronegative groups are favoured for hA_3 affinity, while blue indicates electropositive groups are favoured.

As shown in Figure 4b, a yellow contour was observed at both the *ortho* and *para* positions of the 2-phenyl ring in TQXs, PQs, TPs, and TBTs. The presence of bulky groups was not favourable at these two positions. Particularly, the presence of a bulky NO_2 group at *para* position of the phenyl ring in some of our newly synthesized 2-(*para*-substituted)phenyl pyrazolo-triazolo-pyrimidines[12] as well as in TQX series[17] (e.g., compound **71**, hA_3K_i = 100 nM; compound **89**, hA_3K_i = 655 nM; compound **100**, hA_3K_i = 56.4 nM) has resulted in a considerable decrease of hA_3

Table 1
Structures and hA_3 binding affinities of all reference compounds (*training set*, compounds **1–83**) and testing compounds (*testing* set, compounds **84–105**)

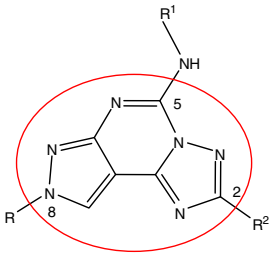

Pyrazolo-triazolo-pyrimidines

(PTP) **1-53, 84-105**

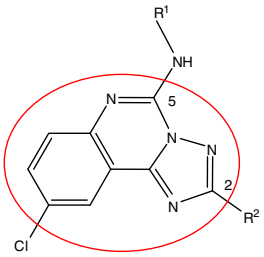

CGS15943 derivatives

54-56

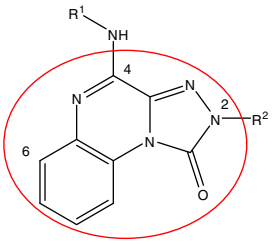

Triazoloquinoxalinones

(TQX) **57-72**

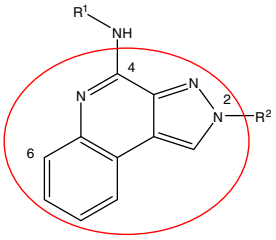

Pyrazoloquinolines

(PQ) **73-75**

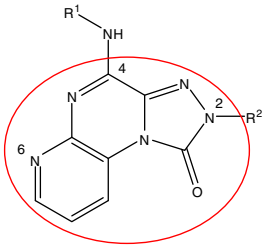

Triazolopyrazinones

(TP) **76-79**

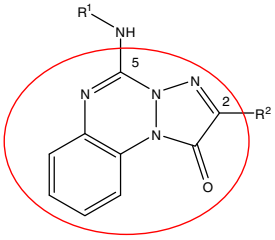

Triazolobenzotriazinones

(TBT) **80-83**

Compounds	R	R^1	R^2	hA_3 (K_i/nM)
1	CH_3	H	Furyl	300
2	CH_3	Ph-NHCO	Furyl	0.16
3	CH_3	4-SO_3H-Ph-NHCO	Furyl	25
4	CH_3	3,4-OCH_2O-Ph-NHCO	Furyl	0.24
5	CH_3	4-NO_2-Ph-NHCO	Furyl	0.43
6	CH_3	4-Br-Ph-NHCO	Furyl	0.46
7	CH_3	4-OMe-Ph-NHCO	Furyl	0.2
8	CH_3	3-Cl-Ph-NHCO	Furyl	0.4
9	CH_3	Pyridine-NHCO	Furyl	0.04
10	CH_3	Pyridinium-NHCO	Furyl	0.01
11	CH_3	Ph-CH_2-CO	Furyl	0.81
12	C_2H_5	H	Furyl	331
13	C_2H_5	Ph-NHCO	Furyl	0.18
14	C_2H_5	4-SO_3H-Ph-NHCO	Furyl	40
15	C_2H_5	3,4-OCH_2O-Ph-NHCO	Furyl	0.27
16	C_2H_5	4-NO_2-Ph-NHCO	Furyl	0.65
17	C_2H_5	4-Br-Ph-NHCO	Furyl	0.37
18	C_2H_5	4-OMe-Ph-NHCO	Furyl	0.6
19	C_2H_5	3-Cl-Ph-NHCO	Furyl	1.6
20	C_2H_5	Ph-CH_2-CO	Furyl	1.03
21	C_3H_7	H	Furyl	408
22	C_3H_7	Ph-NHCO	Furyl	0.15
23	C_3H_7	3,4-OCH_2O-Ph-NHCO	Furyl	0.3
24	C_3H_7	4-NO_2-Ph-NHCO	Furyl	0.81
25	C_3H_7	4-Br-Ph-NHCO	Furyl	0.45
26	C_3H_7	3-Cl-Ph-NHCO	Furyl	0.91
27	C_3H_7	3,4-Cl_2-Ph-NHCO	Furyl	2.5
28	C_3H_7	Ph-CH_2-CO	Furyl	1.01
29	C_4H_9	H	Furyl	600
30	C_4H_9	Ph-NHCO	Furyl	0.21
31	C_4H_9	3,4-OCH_2O-Ph-NHCO	Furyl	0.5
32	C_4H_9	4-NO_2-Ph-NHCO	Furyl	0.55
33	C_4H_9	4-Br-Ph-NHCO	Furyl	0.91
34	C_4H_9	4-OMe-Ph-NHCO	Furyl	0.32
35	C_4H_9	3-Cl-Ph-NHCO	Furyl	0.6
36	C_4H_9	3,4-Cl_2-Ph-NHCO	Furyl	3.7
37	C_4H_9	Ph-CH_2-CO	Furyl	1.11
38	$(CH_3)_2CHCH_2CH_2$	H	Furyl	700
39	$(CH_3)_2CHCH_2CH_2$	Ph-O-CH_2-CO	Furyl	50
40	$(CH_3)_2CHCH_2CH_2$	$(CH_3)_2$CH-NHCO	Furyl	65
41	$PhCH_2CH_2$	H	Furyl	280

Table 1 (*continued*)

Compounds	R	R^1	R^2	hA_3 (K_i/nM)
42	$PhCH_2CH_2$	Ph-CH_2-CO	Furyl	45
43	$PhCH_2CH_2$	Ph-O-CH_2-CO	Furyl	300
44	$PhCH_2CH_2$	α-Napthyl-CH_2-CO	Furyl	120
45	$PhCH_2CH_2$	$NH_3^+CH_2CO$	Furyl	163
46	$PhCH_2CH_2$	$(CH_3)_2$CH-NHCO	Furyl	9.0
47	$PhCH_2CH_2$	$(CH_3)_3$C-NHCO	Furyl	4.9
48	$PhCH_2CH_2CH_2$	H	Furyl	430
49	$PhCH_2CH_2CH_2$	Ph-CH_2-CO	Furyl	121
50	$PhCH_2CH_2CH_2$	Ph-O-CH_2-CO	Furyl	40
51	$PhCH_2CH_2CH_2$	α-Napthyl-CH_2-CO	Furyl	300
52	$PhCH_2CH_2CH_2$	3-Cl-Ph-NHCO	Furyl	60
53	$PhCH_2CH_2CH_2$	$(CH_3)_3$C-NHCO	Furyl	65
54	—	H	Furyl	13.8
55	—	Ph-CO	Furyl	3.03
56	—	Ph-CH_2-CO	Furyl	0.65
57	—	H	3-CH_3-Ph	28.5
58	—	H	4-CH_3-Ph	48.3
59	—	H	3-F-Ph	157
60	—	H	4-Cl-Ph	329
61	—	H	4-OCH_3-Ph	45.3
62	—	Cyclopentyl	Ph	55.4
63	—	Cyclopentyl	3-CH_3-Ph	27.5
64	—	Cyclopentyl	3-F-Ph	173
65	—	Cyclohexyl	4-Cl-Ph	56.1
66	—	CH_3CH_2-CO	Ph	15.8
67	—	Ph-NHCO	Ph	276
68	—	4-OCH_3-Ph-NHCO	Ph	960
69	—	Ph-CO	Ph	1.47
70	—	Ph-CO	4-OCH_3-Ph	2.9
71	—	Ph-CO	4-NO_2-Ph	100
72	—	Ph-CH_2-CO	Ph	3.75
73	—	H	4-OCH_3-Ph	90.2
74	—	Ph-CO	Ph	2.1
75	—	Ph-CO	4-OCH_3-Ph	3.4
76	—	H	4-F-Ph	490
77	—	H	4-OCH_3-Ph	158
78	—	Ph-CO	Ph	70.3
79	—	Ph-CO	4-OCH_3-Ph	4.54
80	—	H	Ph	34.6
81	—	H	4-F-Ph	368.5
82	—	H	4-Cl-Ph	33.2
83	—	H	4-OCH_3-Ph	51.0
84	CH_3	H	Ph	75.0
85	CH_3	H	4-F-Ph	31.4
86	CH_3	H	4-Cl-Ph	72.4
87	CH_3	H	4-Br-Ph	38.6
88	CH_3	H	4-OCH_3-Ph	16.7
89	CH_3	H	4-NO_2-Ph	655
90	$PhCH_2CH_2$	H	Ph	76.7
91	$PhCH_2CH_2$	H	4-F-Ph	50.6
92	$PhCH_2CH_2$	H	4-Cl-Ph	79.7
93	$PhCH_2CH_2$	H	4-Br-Ph	221
94	$PhCH_2CH_2$	H	4-OCH_3-Ph	25.0
95	CH_3	Ph-CO	Ph	5.0
96	CH_3	Ph-CO	4-F-Ph	3.43
97	CH_3	Ph-CO	4-Cl-Ph	2.82
98	CH_3	Ph-CO	4-Br-Ph	5.24
99	CH_3	Ph-CO	4-OCH_3-Ph	2.1
100	CH_3	Ph-CO	4-NO_2-Ph	56.4
101	$PhCH_2CH_2$	Ph-CO	Ph	23.9
102	CH_3	Ph-CH_2-CO	4-Cl-Ph	0.248
103	CH_3	Ph-CH_2-CO	4-Br-Ph	0.345
104	CH_3	Ph-CH_2-CO	4-OCH_3-Ph	0.241
105	$PhCH_2CH_2$	Ph-CH_2-CO	4-Cl-Ph	8.48

affinity as compared to other less bulky *para*-substituents (e.g., compound **85**,. hA_3K_i = 31.4 nM; compound **97**, hA_3K_i = 2.82 nM).

A green contour (Fig. 4a and b) was seen around the phenyl ring at both the N^5- and N^4-positions of the tricyclic nuclei, indicating that bulky groups were tolerable around this region. This was in agreement with previous results and our recent findings, which have shown that introduction of longer chains at N^5- and N^4-positions imparted additional beneficial effects on the hA_3 affinity profile of corresponding derivatives.[12–20,25,26] A small patch of yellow contour was found between the *meta* and *para*-positions of the phenyl ring in PTP derivatives bearing the arylcarbamoyl chain, suggesting that only substituents of a certain size were acceptable

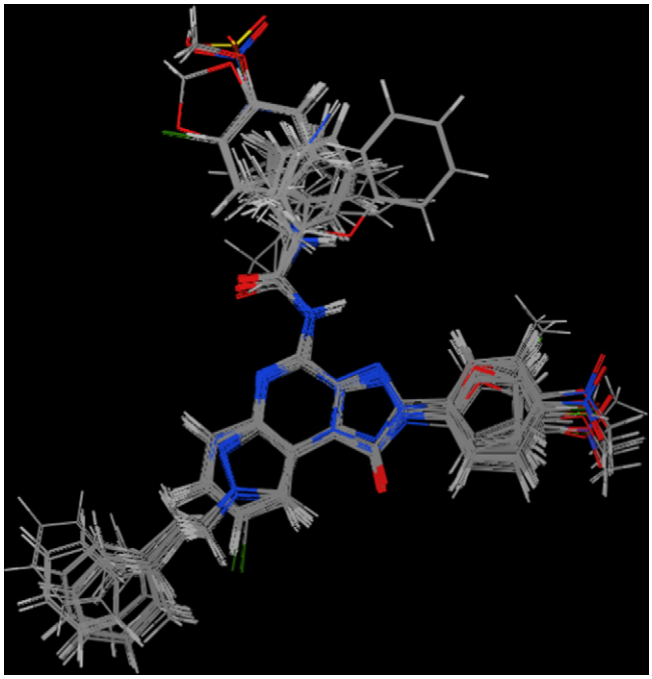

Figure 1. Final structural alignment for 83 compounds in the *training set* and 22 compounds in the *testing set*.

Table 2
Statistical results from CoMFA

Parameters	Statistical values
No. of compounds	83
No. of optimal components	10
q^2 (r^2_{cv})	0.703
r^2	0.936
r^2_{pred}	0.663
F-test	104.782
p-Value	<0.001
Standard error of estimate	0.332
Steric contribution	0.539
Electrostatic contribution	0.461
R_0^2	0.661
$R_0'^2$	0.425
K	0.936
K'	1.061
$(r^2_{pred} - R_0^2)/(r^2_{pred})$	0.00302
$\lvert R_0^2 - R_0'^2 \rvert$	0.236

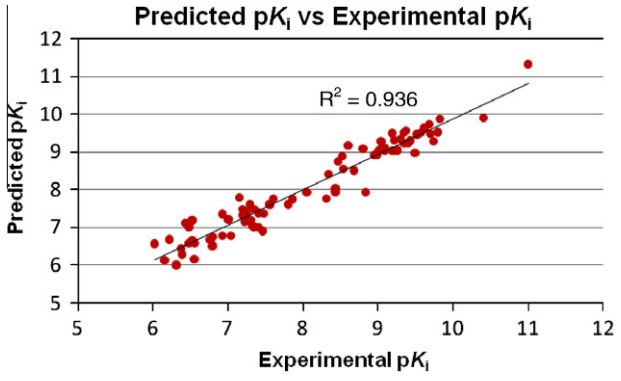

Figure 2. Graphs showing correlation between the predicted pK_i and experimental pK_i of compounds in the *training set*.

at these two positions (Fig. 4a). For example, compound **3** in the *training set* (hA_3K_i = 25 nM) suffered from tremendous decrease of hA_3 affinity due to the presence of a relatively bulky SO_3H group at the *para* position of N^5-phenyl ring, as compared to other polar substitutents. In Moro et al.,[21] it was also reported that a steric control seemed to take place around the *para* and *meta*-position of the phenyl ring at N^5-position of PTPs.

A green contour observed around the substituent at the N^8-position of PTPs (Fig. 4a) implied that incorporation of substituents at this position was preferable to provide good affinity at hA_3 receptors. Nevertheless, a few yellow contours were also observed above and at the immediate left-hand corner of the green contour, suggesting that the presence of bulky groups (such as a phenyl ring), was not suitable at such region. This was in concordance to our observation from the new series of 2-aryl PTP derivatives, in which a relatively less bulky and linear alkyl chain like a methyl group (e.g., compound **95**, hA_3K_i = 5 nM), was more favorable at the N^8 position as compared to the bulky alkyl chains such as phenylethyl group (e.g., compound **101**, hA_3K_i = 23.9 nM).[12] Undeniably, an inverse relationship has been established between the binding affinity values at hA_3 receptor and the molecular volume (MV) of the substituent at position N^8: The higher the MV, the lower the affinity towards the hA_3 receptor.[12,13] Besides that, a green contour was also seen in vicinity to the 6-position of phenyl ring in TQXs (Fig. 4b), PQs, and TPs, as well as 7-position of phenyl ring in CGS derivatives and TBTs. Bulky groups seemed to accommodate better at this particular position. As reported in Lenzi et al.,[17] bulky polar substituents such as NO_2 groups were introduced at 6-position of the phenyl ring in some of the TQX derivatives, which displayed good affinity towards the hA_3 receptors.

A blue contour was observed in proximity of the phenyl ring and the furan ring at the C^2 or N^2-position of the tricyclic nucleus (Fig. 4a and b). It was believed that delocalization of electrons towards the pseudoaromatic tricyclic core has exerted its effect on the phenyl and furan rings, thus rendering the surrounding region to be more electron-deficient. According to previously reported results, the presence of either furan ring in PTPs and CGS derivatives or phenyl ring in TQXs, PQs, TPs, and TBTs seemed essential to maintain affinity at the hA_3 receptors.[13–20,25] In our recent study, we found that the substitution of the furan ring in PTP derivatives with a (un)substituted-phenyl ring (compounds **84–105**), indeed conferred better affinity and selectivity profile in comparison to that of 2-furyl counterparts (3–7-folds increase of hA_3 affinity and significant improvement in selectivity of 2–3 order of magnitude).[12]

A red contour was found around the –CONH group at the N^5- and N^4-position of the tricyclic nuclei, indicating that the presence of an electronegative group (e.g., carbonyl group) was favoured for hA_3 affinity (Fig. 4a and b). This was in accordance with previous studies[13–15,25] and with our recent findings,[12] which demonstrated that the N^4-substituted TQXs,[16,17] PQs[18] and TPs[19] (with amidic chain) as well as the N^5-substituted PTP and CGS15943 derivatives (with arylcarbamidic or amidic chain) presented a remarkable improvement in hA_3 affinity. Around the phenyl ring at the N^5- and N^4-position, a blue contour was noticed. Similar to that of C^2-phenyl ring, the electron-withdrawing effect of *para*-substituents or delocalization of electrons towards the nearby carbamoyl and amidic group caused the phenyl ring to be electron-deficient. Consistently, a red contour was observed at the *para*-position of such N^5-phenyl ring in the PTP derivatives (e.g., compound **3** in Fig. 4a). This observation was further substantiated by the good hA_3 affinity profile ranging from 0.2 to 0.4 nM as demonstrated, for examples, by compounds **4–7**, which bear electronegative groups at the *para* position.

A red contour was also observed at the N^7 of the pyrazole in PTPs (Fig. 4a) and 6-position of the phenyl ring in TQXs and PQs

Table 3
hA_3 binding affinities (pK_i) (observed, predicted and residual) of newly synthesized 2-(*para*-(un)substituted)phenyl-pyrazolo-triazolo-pyrimidine derivatives

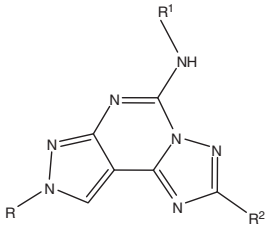

***Testing compounds*, 84-105**

Compds	R	R^1	R^2	hA_3 (pK_i)		
				Observed	Predicted	Residual[a]
84	CH_3	H	Ph	7.125	6.394	−0.731
85	CH_3	H	4-F-Ph	7.503	7.003	−0.500
86	CH_3	H	4-Cl-Ph	7.140	7.285	0.145
87	CH_3	H	4-Br-Ph	7.413	7.511	0.098
88	CH_3	H	4-OCH_3-Ph	7.777	7.189	−0.588
89	CH_3	H	4-NO_2-Ph	6.184	5.931	−0.253
90	$PhCH_2CH_2$	H	Ph	7.115	5.769	−1.346
91	$PhCH_2CH_2$	H	4-F-Ph	7.296	5.757	−1.539
92	$PhCH_2CH_2$	H	4-Cl-Ph	7.099	6.029	−1.070
93	$PhCH_2CH_2$	H	4-Br-Ph	6.656	5.854	−0.802
94	$PhCH_2CH_2$	H	4-OCH_3-Ph	7.602	6.144	−1.458
95	CH_3	Ph-CO	Ph	8.301	8.021	−0.280
96	CH_3	Ph-CO	4-F-Ph	8.465	8.687	0.222
97	CH_3	Ph-CO	4-Cl-Ph	8.55	8.836	0.286
98	CH_3	Ph-CO	4-Br-Ph	8.281	8.982	0.701
99	CH_3	Ph-CO	4-OCH_3-Ph	8.678	8.577	−0.101
100	CH_3	Ph-CO	4-NO_2-Ph	7.249	7.829	0.580
101	$PhCH_2CH_2$	Ph-CO	Ph	7.622	7.167	−0.455
102	CH_3	Ph-CH_2-CO	4-Cl-Ph	9.606	8.539	−1.067
103	CH_3	Ph-CH_2-CO	4-Br-Ph	9.462	8.559	−0.903
104	CH_3	Ph-CH_2-CO	4-OCH_3-Ph	9.618	8.646	−0.972
105	$PhCH_2CH_2$	Ph-CH_2-CO	4-Cl-Ph	8.072	6.869	−1.203

[a] Residual refers to the corresponding difference between the predicted and observed pK_i.

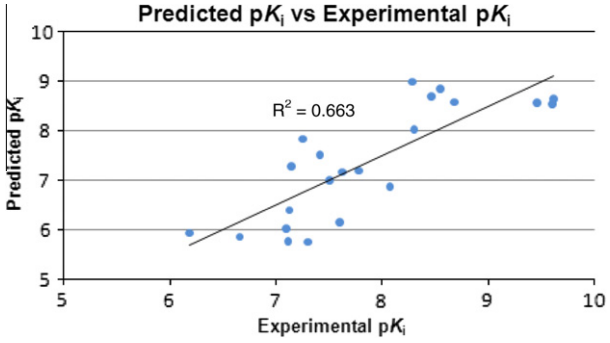

Figure 3. Graphs showing correlation between the predicted pK_i and experimental pK_i of compounds in the *testing set*.

(Fig. 4b), as well as 7-position of the phenyl ring in CGS derivatives and TBTs. In fact, electronegative substituents (such as NO_2 group) were previously introduced at 6-position of phenyl ring in TQX series, which resulted in improvement of hA_3 affinity.[17] Subsequently, the sp^2 carbon atom at 6-position was replaced with a corresponding sp^2 nitrogen atom, as represented by TP derivatives.[19] Notably, this new series of TP derivatives also showed good affinity profile at the hA_3 receptors. On the other hand, a relatively small blue contour was observed near the substituents at the N^8-position of PTPs. The electrostatic effect at this position seemed negligible; instead, the steric effect at this position was expected to determine a more important role towards the hA_3 affinity, as elaborated in the previous section.

In general, there are some differences between our CoMFA pharmacophore model and the contour maps reported by Moro et al.[21] Apart from the additional ability to identify the steric and electrostatic effects at the C^2-position of PTPs, our model highlighted the presence of green and yellow contour plots at the N^8-position, as well as the red contour plot at the N^7-position. Notably, these were not elaborated in the latter model. Furthermore, it was also found that the electrostatic effect at the N^8-position seemed negligible in our study, which was in contrast to the findings by Moro et al. that described the significance of red polyhedron at such position.

To further support our CoMFA model, the obtained contour plots were also compared with the docking results of the 2-aryl PTPs within the putative binding site of a hA_3AR complex built on the hA_{2A} crystal structure.[12] The projection of the corresponding contour maps onto the putative antagonist-binding site, which was validated by the experimental SAR profiles, displayed good complementarity. In relative to the large and hydrophobic N^5-phenyl ring (delineated by green and blue contour plots) close to the extracellular loop 2 (ECL2), the binding site of the N^8-position (delineated by yellow contour plots) appeared to be of restricted space and was directed towards the inner transmembrane (TM) re-

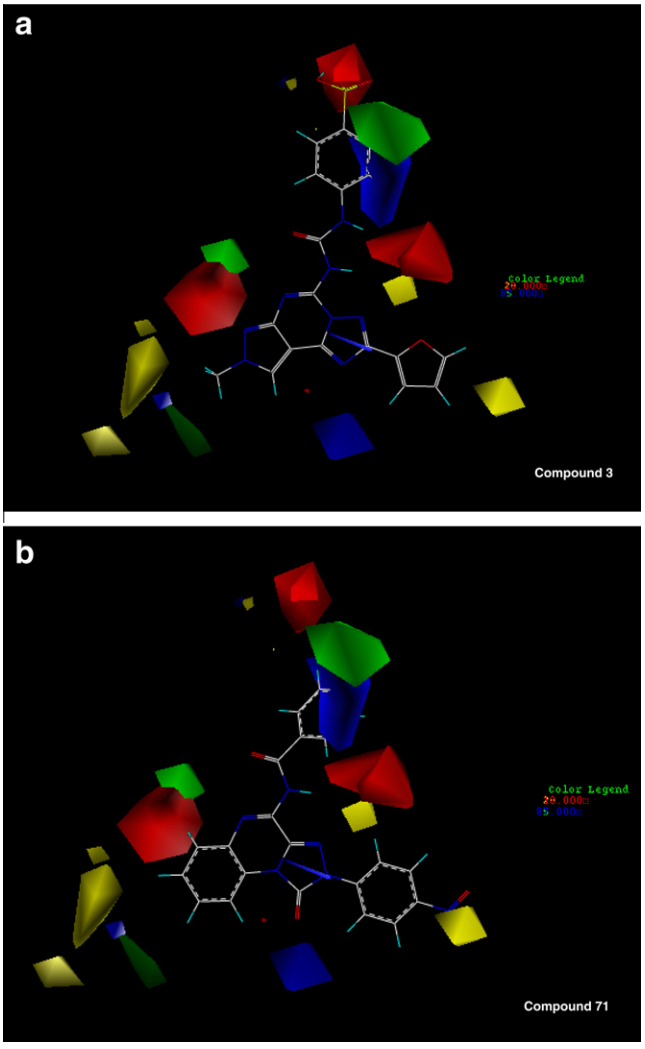

Figure 4. Combined steric and electrostatic contour plots for (a) compound **3** and (b) compound **71**. Green color indicates bulky groups are favoured, and yellow indicates bulky groups are disfavoured; red indicates electronegative groups are favoured, and blue indicates electropositive groups are favoured. Contour plot's color legend threshold: green/yellow 85/20; blue/red 87/18.

gion. The blue contour plot near to the 2-aryl ring was surrounded by non-polar residues at TM2; on the other hand, the two red contour plots around the N^5-amino/amidic groups and N^7-position were complementary to the interaction with neighbouring Asn250 residue.

In conclusion, the QSAR study based on CoMFA has provided new insights on the steric and electrostatic factors that are important in modulating the hA_3 affinity for the new series of 2-aryl PTP derivatives, particularly at the C^2-position of the tricyclic nucleus (as illustrated by compound **104** in Fig. 5). On top of that, a predictive QSAR model was also obtained, which was able to predict the hA_3 affinities of these new 2-aryl PTPs with appreciable accuracy. In general, the distribution of steric and electrostatic effects in the PTP system are as follows: (a) The steric effect is prominent at the N^5- and N^8-positions as well as at the *para*-position of 2-phenyl ring; bulky groups are unfavourable at both the N^8-position and *para*-position of 2-phenyl ring, while bulky groups are preferable at the N^5-position of the tricyclic nucleus. (b) For the electrostatic effect, the presence of electronegative groups seems favourable around the amidic group at N^5, at the *para*-position of N^5-phenyl ring on arylcarbamoyl moiety and sp^2 N^7 on pyrazolo ring, whereas the electropositive group is preferred around the

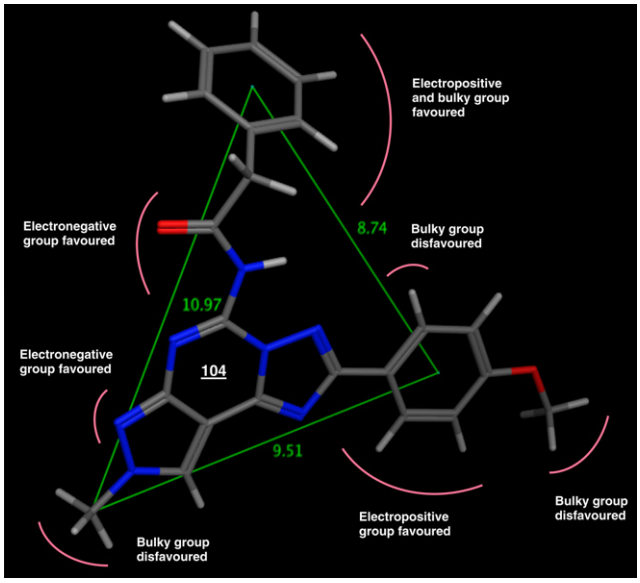

Figure 5. Distribution of steric and electrostatic effects in the 2-aryl pyrazolo-triazolo-pyrimidine derivative, compound **104**. The distances (Å) among the three pharmacophoric points constituted by the N^5-phenyl ring, N^8-methyl and C^2-aryl ring are indicated. Conformation of the structure is obtained from the final alignment shown in Figure 1. Red atom: oxygen; blue atom: nitrogen; dark grey atom: carbon; light grey atom: hydrogen.

C^2- and N^5-positions. Overall, the contribution of the steric effect was found relatively more predominant for the optimal interaction of these antagonists to the hA_3 receptor.

Acknowledgments

This work has been supported by the National University of Singapore (FRC grant, R-148-000-129-112) and A-STAR (TSRP project, R-148-001-435-305).

Supplementary data

Supplementary data (experimental information related to the CoMFA) associated with this article can be found, in the online version, at doi:10.1016/j.bmcl.2011.03.073.

References and notes

1. Jacobson, K. A.; Gao, Z. G. *Nat. Rev. Drug Disc.* **2006**, *5*, 247.
2. Moro, S.; Gao, Z. G.; Jacobson, K. A.; Spalluto, G. *Med. Res. Rev.* **2006**, *26*, 131.
3. Cosyn, L.; Krishnan, K.; Palaniappan, K. K.; Kim, S. K.; Duong, H. T.; Gao, Z. G.; Jacobson, K. A.; Calenbergh, S. V. *J. Med. Chem.* **2006**, *49*, 7373.
4. Abbracchio, M. P.; Brambilla, R.; Ceruti, S.; Kim, H. O.; von Lubitz, D. K.; Jacobson, K. A.; Cattabeni, F. *Mol. Pharmacol.* **1995**, *48*, 1038.
5. Haas, H. L.; Selbach, O. *Naunyn-Schmiedeberg's Arch. Pharmacol.* **2000**, *362*, 375.
6. von Lubitz, D. K.; Ye, W.; McClellan, J.; Lin, R. C. *Ann. N.Y. Acad. Sci.* **1999**, *890*, 93.
7. Shryock, J. C.; Belardinelli, L. *Am. J. Cardiol.* **1997**, *79*, 2.
8. Jacobson, K. A. *Trends Pharmacol. Sci.* **1998**, *19*, 184.
9. Merighi, S.; Mirandola, P.; Varani, K.; Gessi, S.; Leung, E.; Baraldi, P. G.; Tabrizi, M. A.; Borea, P. A. *Pharmacol. Ther.* **2003**, *100*, 31.
10. Baraldi, P. G.; Cacciari, B.; Romagnoli, R.; Borea, P. A.; Varani, K.; Pastorin, G.; Da Ros, T.; Tabrizi, M. A.; Fruttarolo, F.; Spalluto, G. *Curr. Pharm. Des.* **2002**, *8*, 2299.
11. Baraldi, P. G.; Cacciari, B.; Romagnoli, R.; Klotz, K. N.; Spalluto, G.; Varani, K.; Gessi, S.; Merighi, S.; Borea, P. A. *Drug Dev. Res.* **2001**, *53*, 225.
12. Cheong, S. L.; Dolzhenko, A.; Kachler, S.; Paoletta, S.; Federico, S.; Cacciari, B.; Dolzhenko, A.; Klotz, K. N.; Moro, S.; Spalluto, G.; Pastorin, G. *J. Med. Chem.* **2010**, *53*, 3361.
13. Baraldi, P. G.; Cacciari, B.; Romagnoli, R.; Spalluto, G.; Moro, S.; Klotz, K. N.; Leung, E.; Varani, K.; Gessi, S.; Merighi, S.; Borea, P. A. *J. Med. Chem.* **2000**, *43*, 4768.
14. Baraldi, P. G.; Cacciari, B.; Moro, S.; Spalluto, G.; Pastorin, G.; Da Ros, T.; Klotz, K. N.; Varani, K.; Gessi, S.; Borea, P. A. *J. Med. Chem.* **2002**, *45*, 770.
15. Kim, Y.-C.; Ji, X.-D.; Jacobson, K. A. *J. Med. Chem.* **1996**, *39*, 4142.

16. Colotta, V.; Catarzi, D.; Varano, F.; Cecchi, L.; Filacchioni, G.; Martini, C.; Trincavelli, L.; Lucacchini, A. *J. Med. Chem.* **2000**, *43*, 1158.
17. Lenzi, O.; Colotta, V.; Catarzi, D.; Varano, F.; Filacchioni, G.; Martini, C.; Trincavelli, L.; Ciampi, O.; Varani, K.; Marighetti, F.; Morizzo, E.; Moro, S. *J. Med. Chem.* **2006**, *49*, 3916.
18. Colotta, V.; Catarzi, D.; Varano, F.; Capelli, F.; Lenzi, O.; Filacchioni, G.; Martini, C.; Trincavelli, L.; Ciampi, O.; Pugliese, A. M.; Pedata, F.; Schiesaro, A.; Morizzo, E.; Moro, S. *J. Med. Chem.* **2007**, *50*, 4061.
19. Colotta, V.; Lenzi, O.; Catarzi, D.; Varano, F.; Filacchioni, G.; Martini, C.; Trincavelli, L.; Ciampi, O.; Pugliese, A. M.; Traini, C.; Pedata, F.; Morizzo, E.; Moro, S. *J. Med. Chem.* **2009**, *52*, 2407.
20. Da Settimo, F.; Primofiore, G.; Taliani, S.; Marini, A. M.; La Motta, C.; Simorini, F.; Salerno, S.; Sergianni, V.; Tuccinardi, T.; Martinelli, A.; Cosimelli, B.; Greco, G.; Novellino, E.; Ciampi, O.; Trincavelli, M. L.; Martini, C. *J. Med. Chem.* **2007**, *50*, 5676.
21. Moro, S.; Braiuca, P.; Deflorian, F.; Ferrari, C.; Pastorin, G.; Cacciari, B.; Baraldi, P. G.; Varani, K.; Borea, P. A.; Spalluto, G. *J. Med. Chem.* **2005**, *48*, 152.
22. Costantino, G.; Macchiarulo, A.; Camaioni, E.; Pellicciari, R. *J. Med. Chem.* **2001**, *44*, 3786.
23. Tropsha, A.; Golbraikh, A. *Curr. Pharm. Des.* **2007**, *13*, 3494.
24. Golbraikh, A.; Tropsha, A. *J. Mol. Graphics Modell.* **2002**, *20*, 269.
25. Baraldi, P. G.; Tabrizi, M. A.; Bovero, A.; Avitabile, B.; Preti, D.; Fruttarolo, F.; Romagnoli, R.; Varani, K.; Borea, P. A. *Eur. J. Med. Chem.* **2003**, *38*, 367.
26. Colotta, V.; Catarzi, D.; Varano, F.; Calabri, F. R.; Lenzi, O.; Filacchioni, G.; Martini, C.; Trincavelli, L.; Deflorian, F.; Moro, S. *J. Med. Chem.* **2004**, *47*, 3580.